

**GEOLOGICAL SURVEY OF CANADA**

**OPEN FILE 1994**

**AGASSIZ METALLOTECT: APPLICATION OF MEIS-II FOR  
BIOGEOCHEMICAL REMOTE SENSING AND GEOCHEMICAL  
EXPLORATION**

**(LYNN LAKE, MANITOBA)**

**Vijay Singh, Wooil M. Moon, and Mark Fedikow**

This document was produced  
by scanning the original publication.

Ce document a été produit par  
numérisation de la publication originale.

**1989**



Energy, Mines and  
Resources Canada

Énergie, Mines et  
Ressources Canada

**Canada**

# MINERALS

## ECONOMIC & REGIONAL DEVELOPMENT AGREEMENT

Geological Survey of Canada

**AGASSIZ METALLOTECT: APPLICATION OF MEIS-II FOR  
BIOGEOCHEMICAL REMOTE SENSING AND GEOCHEMICAL  
EXPLORATION**

**(LYNN LAKE, MANITOBA)**

**Vijay Singh and Woil M. Moon**

Department of Geological Sciences  
The University of Manitoba  
Winnipeg, Canada R3T 2N2

**Mark Fedikow**

Geological Services  
Department of Energy and Mines  
Province of Manitoba  
Winnipeg, Canada R3C 4E3

Contribution to Canada-Manitoba Mineral Development Agreement 1984-89, a subsidiary agreement under the Economic and Regional Development Agreement. Project funded by the Geological Survey of Canada.

Manitoba  
Energy and Mines



GSC OPEN FILE  
1994

Energy, Mines and  
Resources Canada

Énergie, Mines et  
Ressources Canada

MAY, 1989

Canada

Manitoba



## INTRODUCTION

A number of remote sensing techniques have been applied in conjunction with the geobotanical approach to identify mineralized zones (Collins et al., 1983; Labovitz et al., 1983; Milton, 1983; Lulla, 1985). Some of the earlier attempts were the use of aerial photography which provided high spatial resolution. Colour aerial photography further aids in discriminating the earth materials because the photographic images appear as the human eye perceives them. False colour infrared photographs have been used with success, because the vegetation is most reflective in the infrared parts of the spectrum. Thus some of the changes in optical and/or thermal reflectance which are not noticeable to human eye can be distinguished.

In late 1970's and early 1980's Landsat Multispectral Scanner (MSS) and Landsat Thematic Mapper (TM) have been applied to detect geobotanical anomalies associated with economic mineral deposits (Goetz et al., 1983). Landsat MSS and Landsat TM record the spectral information of the scene in different spectral bands. The spectral reflectance properties of a leaf (in the region 0.4 to 2.5  $\mu\text{m}$ ) are functions of the leaf pigments, primarily the chlorophyll pigments, the leaf cell internal refractive index discontinuities, and water content (Goetz et al., 1983).

The airborne spectral remote sensing data offer an advantage over the aerial photography and Landsat imagery, because it allows the same area to be covered by more than one band in the electromagnetic spectrum. The data are collected through the use of electro-optical devices which detect variations in either reflected, emitted or both from the terrain features within selected regions of the electromagnetic spectrum. The ability to operate throughout this broad spectral region represents the possibility of identifying target regions whose identifiable 'signatures' lie beyond the limits of the relatively narrow portion of the visible spectrum.

Geochemical and biogeochemical techniques have been used successfully in the past for exploration of mineral deposits (Hawkes and Webb, 1962; Cameron, 1966; Boyle and McGerrigle, 1971; Brooks, 1972, 1983). The geochemical techniques are based on the fact that materials of the earth around a mineral deposit, that is rocks, soils, streams, lake sediments, and water, may be expected to differ in chemical composition from similar materials where there is no mineral deposit present. Thus the operational procedures of exploration geochemistry require that one or more types of the earth materials (rock, soil, sediment, or water) be sampled and chemically analysed for one or more elements in an attempt to recognize an anomalous element distribution pattern, which may be related to a mineral deposit. The choice of the material is dictated to some extent by the local availability.

The basis of biogeochemical exploration is the relationship between plant nutrient requirements and other factors related to the availability of nutrients in the soil and the physical properties of the soils, including the soil moisture. However, implicit to the application of biogeochemical exploration is the assumption that there is some relation between the soils and the underlying rocks. The amounts of nutrients present in the soil is a function of the soil forming process and the amount of nutrients present in the parent rock material. But all of the contained nutrients are not necessarily available to the plants, and this is dependent on the physical and chemical properties of the soil.

Nutrients and toxic metals tend to move toward the actively growing cells in the branch tips, root tips, and green foliage. It is not known by what physical and chemical mechanisms the metals or metal complexes interfere with normal plant growth, but they are known to cause chlorotic leaves (leaves which have low chlorophyll contents), stunted or oversized growth, abnormal blossoms or seeds, and other visible signs of poor health or altered development (Brooks, 1972, 1983).

Geobotanical exploration involves the observation and analysis of these anomalous morphological and colour features as well as the anomalous distribution of plant species.

The detection of plants under stress, especially stress related to an excess concentration of metal ions is geologically significant. The chlorophyll pigments are generally believed to be the parts of the plant most sensitive to the various types of stress (Bolviken et al., 1977; and Brooks, 1983). Therefore, in the electromagnetic spectrum, the chlorophyll absorption bands are thought to be the most sensitive indicators of the stress. A stressful environment, adversely affects the chlorophyll and thus tends to decrease the vigour of growth. In this situation, the leaves may be smaller, less abundant, oriented differently, or other growth related phenomena may occur. All these factors generally affect the leaf area index, which is defined as the ratio of total area of plant canopy to the ground area in the field of view (Brooks, 1983).

In this study the feasibility of airborne multi-detector electro-optical imaging scanner (MEIS-II) and multispectral scanner (MSS) data has been evaluated to determine the signs of vegetation stress, as well as their use as a potential biogeochemical exploration technique.

## STUDY AREA

The study area is centered at Farley Lake, in northern Manitoba (Figure 1). It covers an approximate area of 22 square km, from latitude 100°22'W to 100°28'W and longitude 56°53'N to 56°55'N. This is about 45 km east-northeast of the Lynn Lake town site. It lies a few miles north of the provincial road 391. The following factors influenced the selection of this area for study.

1. The Farley Lake area forms a part of the Agassiz Metallotect, which is a zone about 70 km long of coincident magnetic and electromagnetic anomalies (Fedikow and Gale, 1982; and Fedikow, 1983).
2. It has economic potential; a gold deposit is currently undergoing evaluation.
3. The bedrock geology and stratigraphy at the Farley Lake area are similar to those at the producing gold-silver MacLellan deposit (formerly Agassiz deposit), located about 37 km to the east in the Metallotect.
4. The basal till geochemical and biogeochemical data bases are available for this area in greater detail than for any other area along the Metallotect.
5. Low altitude, high resolution MEIS-II and MSS remote sensing data along with other types of geophysical data are available for the Farley Lake area.

## PURPOSE AND SCOPE OF THE STUDY

As the supplies of easily exploitable mineral deposits are being exhausted there is a definite need to refine and integrate mineral exploration techniques in order to detect new mineral deposits which are difficult to locate with existing exploration methods. Many of the unexplored deposits are covered by thick vegetation, and glacial/soil overburden. Furthermore, about 30 percent of the earth's surface is covered by vegetation, and any method incorporating the use of vegetation in exploration of mineral deposits would have a substantial economic impact. However, such large areas can be explored very effectively by using remote sensing techniques

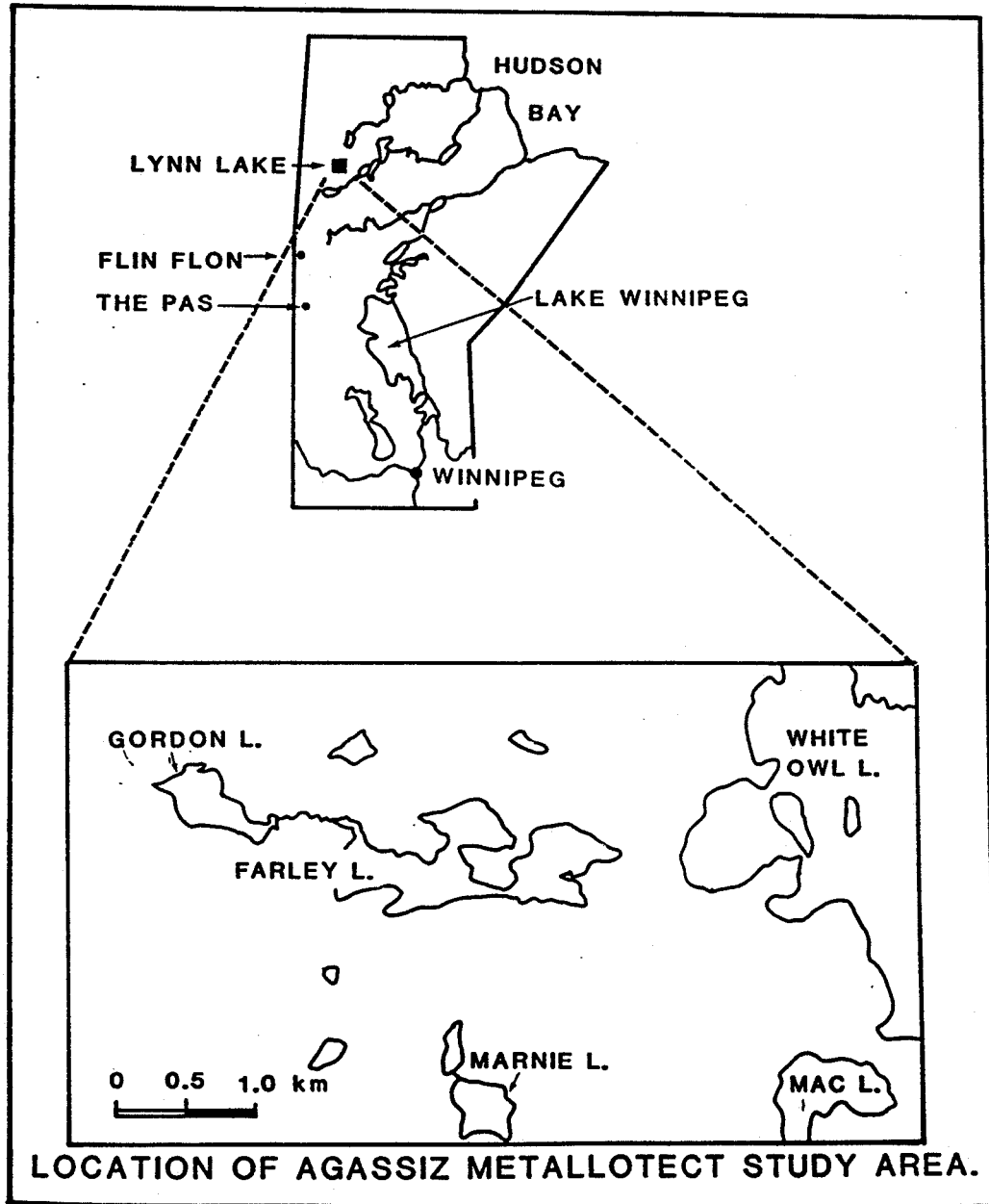


Figure 1. Location of the Farley Lake area, Manitoba.

in conjunction with the use of vegetation. The remote sensing techniques are cost effective due to the following reasons:

1. Airborne and/or satellite borne remote sensing techniques can cover large areas in short intervals of time.
2. Most of the remote sensing data are in digital format, and therefore data storage, retrieval, manipulation, and processing are relatively easy.
3. Remote sensing data can be obtained in different spectral bands and therefore changes that are not obvious to the human eye can be detected more easily.
4. Multitemporal data can be obtained to detect changes in the vegetation with the lapse of time, which may be significant in terms of mineral exploration.

However, most of the present day information about exploration of mineral deposits is obtained from Landsat data. When this Landsat information is used in conjunction with the geobotanical or biogeochemical data, it has the following limitations:

1. The spectral bands for the Landsat sensors are fixed and have a limited resolution. The same spectral windows can not be used over large areas that have different types of vegetation cover.
2. The spatial resolution of the Landsat data is very poor, and it is difficult to resolve many of the features which could serve as important exploration guides.

However, progress in remote sensing techniques for mineral exploration has been made using sensors which employ higher spectral and spatial resolution. In this study airborne multi-detector electro-optical imaging scanner (MEIS-II) and multispectral scanner (MSS) data have been tested. MEIS-II data offer the above described useful characteristics of the Landsat sensors but with improved spectral and spatial resolution. Moreover, the narrow adjustable spectral windows of the airborne MEIS-II and MSS may provide better spectral signatures which are more sensitive to vegetation stress. Spectral filters for MEIS-II can be easily changed and thus optimum spectral band combinations may be readily obtained. The airborne sensors also allow fast and temporal coverage of the area. It is expected that mineralized areas may display some unique spectral variations with the narrow filters in the MEIS-II data, and thus any type of favourable result can provide a new exploration capability. The objectives of this study are as follows:

1. Determine the feasibility of airborne MEIS-II and MSS remote sensing techniques which can be used as an aid for mineral exploration in areas covered with extensive vegetation and glacial overburden.
2. Integration of different types of data, namely, geophysical, geochemical, biogeochemical, and remote sensing.
3. Interpret the relationship among the concentration of different elements in the till and plant ash samples, and their relationship with remotely sensed information.

## **AIRBORNE MEIS-II AND MSS SYSTEM**

### **Multispectral Scanner (MSS) Data**

Multispectral Scanner (MSS) data are collected by using an electro-optical mechanical scanning device. It consists of a rotating mirror which views the ground as a series of narrow ground strips at right angles to the flight line. The forward

motion of the aircraft results in the new ground strips being covered by successive scan lines, thus building up a two-dimensional record of the reflectance information.

### **Multi-detector electro-optical imaging scanner (MEIS-II) Data**

The Multi-detector electro-optical imaging scanner (MEIS-II) uses a push-broom scanner, rather than a scanning mirror, and offers a high spatial and spectral resolution. A push-broom scanner employs a number of very small detectors (CCDs). The detector elements are closely packed in a one-dimensional linear array orthogonal to the flight path. The forward motion of the platform sweeps the linear array of detectors across the ground scene being imaged. Electronic sampling of the across track provides the orthogonal component to form an image, and the aircraft motion along its flight path produces successive lines of image.

Some of the advantages of the MEIS-II data acquisition system over the MSS include the following: (i) improved radiometric sensitivity due to the large detector dwell time on each ground resolution cell, resulting in a high signal to noise ratio, (ii) high geometric accuracy in the across-track direction because of the fixed geometry of the detector arrays. The primary disadvantage is that a very large number of detectors is involved, which means that calibration is difficult and signal level correction presents a real processing burden (Norwood and Lansing, 1983).

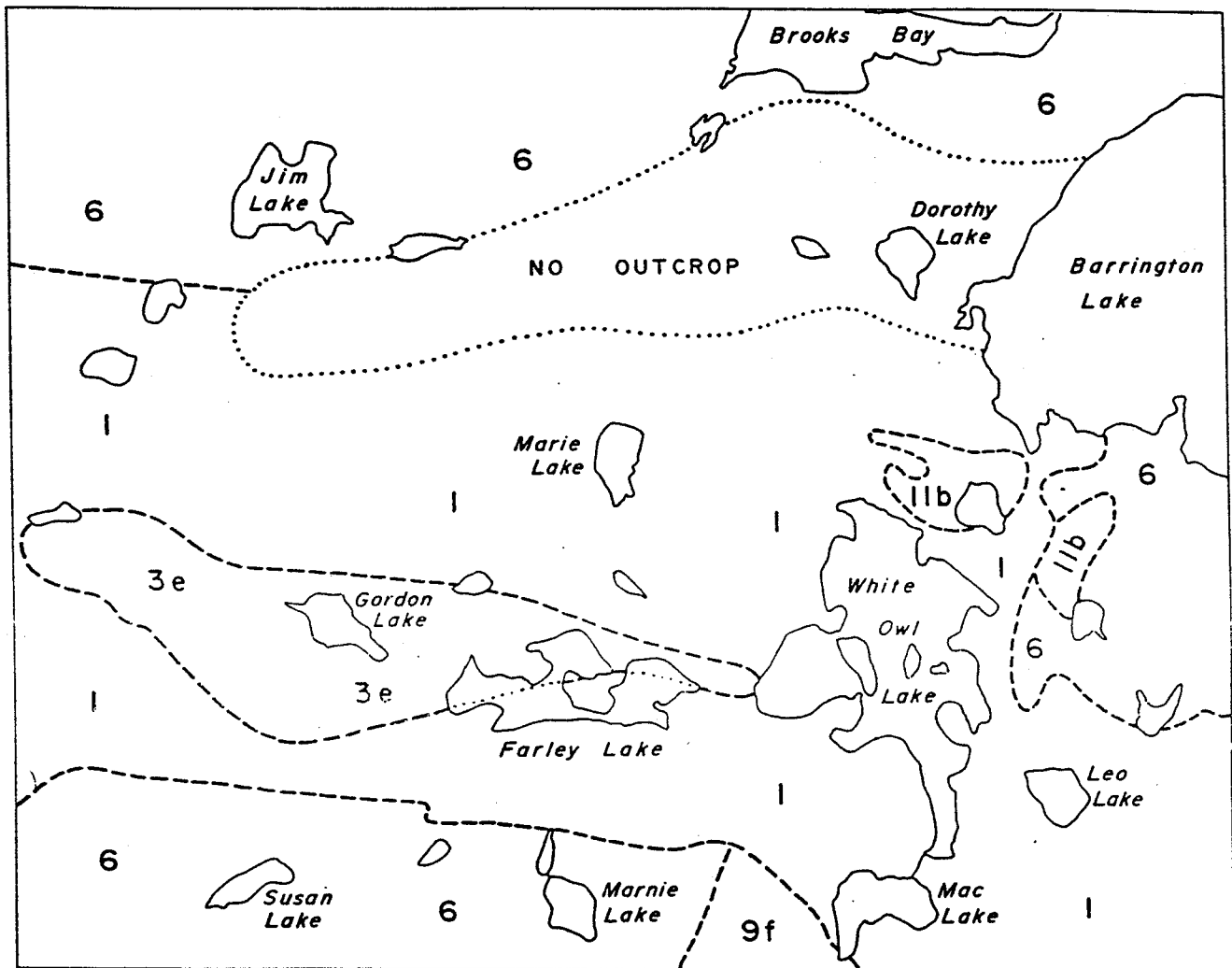
## **GEOLOGICAL SETTING**

The study area is located in the northern part of the Lynn lake greenstone belt. This belt is a complex sequence of metamorphosed volcanic, sedimentary, and plutonic rocks of Proterozoic Aphebian age, that have been assigned to the Wasekwan Group (Bateman, 1945). The Lynn Lake greenstone belt extends for approximately 130 km along its east-west strike, and has a maximum width of about 60 km. The rocks of the Wasekwan Group are unconformably overlain by a sandstone and conglomerate sequence of the Sickie Group. This belt is located in the middle of a larger lithostructural belt extending for approximately 500 km from La Ronge, Saskatchewan (Johnson, 1979) towards the northeast to Partridge Breast Lake, Manitoba (Corkery and Lenton, 1979).

### **Bedrock Geology**

The bedrock geology of the Lynn Lake greenstone belt has been mapped and described by Gilbert et al. (1980). It has been divided into two distinct structural sub-belts, a 'northern belt', which is separated by large granitic intrusions from the 'southern belt'. Lithologically, the 'northern belt' is predominantly composed of mafic volcanic rocks with intercalations of felsic and intermediate rocks; whereas the 'southern belt' is made up of a thick sequence of tholeiitic, aphyric and porphyritic basalts capped by felsic to mafic rocks (Fedikow, 1986).

At Farley Lake, the bedrock is composed of mafic to intermediate volcanic flows, flow breccias, mafic tuffs, and pyroclastic breccias (Figure 2). Small subvolcanic plutons of granitic to tonolitic composition are also present in the area. Gordon and Farley Lakes are situated in a body of iron formation, which consists of banded chert, argillite, siltstone, and massive magnetite. The iron formation is interbedded with a characteristic high Mg-Ni-Cr basalt. This iron formation gives rise to a magnetic anomaly that is about 6.3 km long and 1.5 km wide. The airborne electromagnetic and vertical field magnetic gradiometric anomalies which extend roughly east-west



**Legend**

- 11b Amphibolite
- 9f Granite
- 6 Tonalite
- 3e Magnetite-Chert-Argillite Iron Formation
- 1 Mafic Volcanic Flows and Fragmental Rocks

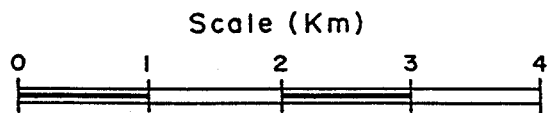


**Figure 2.** Bedrock geology of the Farley Lake area, Manitoba (after, Nielson and Graham, 1985).



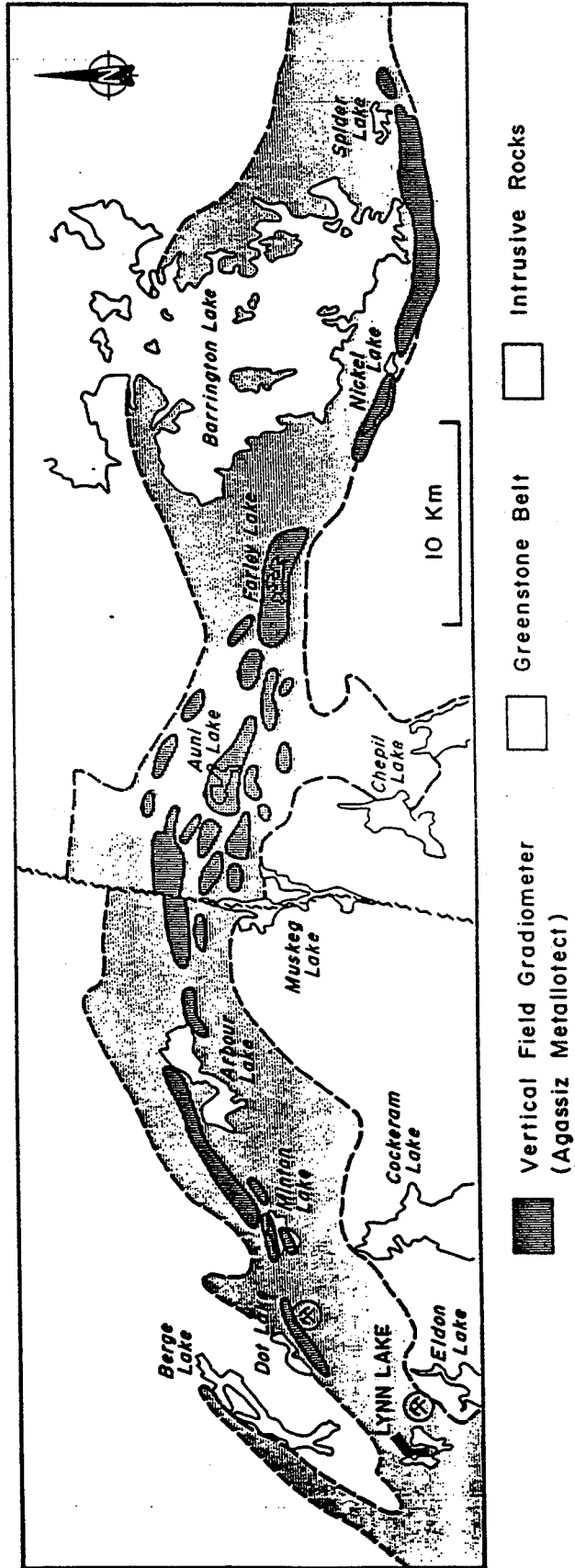


Figure 3. Agassiz Metallotect showing location of vertical field gradiometer anomalies (after Nielson and Graham, (1985).

were used in conjunction with the geological investigation to delineate the Agassiz Metallotect (Figure 3). Fedikow (1986) states that the iron formation, which is interlayered with high Mg-Ni-Cr basalt and siltstone, forms the main component of the Metallotect, as it is observed throughout the Metallotect, and appears to be a unique and well defined sequence in this area. However, some facies changes do occur in the iron formation.

The lithology and stratigraphic sequence of the iron formation in the Farley Lake area is significant because a similar sequence is observed at the producing MacLellan gold-silver deposit to the west. It is possible to extend the stratigraphic sequence to the east from the MacLellan deposit through Farley Lake to Nickel Lake and Barrington Lake (Nielson and Fedikow, 1986). The stratigraphic sequence thickens considerably at the Farley Lake, and within these units strata-bound gold deposits have been discovered near Dot Lake and are currently being investigated between Gordon Lake and Farley Lake. To the south of Farley Lake, mafic volcanic rocks are silicified and interlayered with amphibolite schist.

### Surficial Geology

The area around Farley Lake is of low relief, and lakes in the study area are surrounded by swamps along most of their shores. There is relatively little bedrock exposed in the area (Figure 4). Surficial deposits are of glacial or post-glacial origin, and consist of glacial till, glaciolacustrine silt and clay of glacial Lake Agassiz, and littoral deposits of sand and gravel. More than 60 percent of the area is covered by fen and bog veneer (Nielson and Graham, 1985).

The Lynn Lake region including the Farley Lake area was affected by glaciation from the Laurentide Ice Sheet. The main ice flow direction in the region varies between 180° to 225°, however, in the Farley Lake area the main ice flow was toward 190°, followed by a younger flow toward 140° (Nielson and Graham, 1985). The ice advance was responsible for depositing the till deposits and creating trace metal deposition fans and dispersion trains around areas of known mineralization (Fedikow, 1984). The till sheet is of variable thickness and covers the bedrock; it ranges from no cover over the bedrock highs to a few metres in thickness. Till is generally homogeneous with sandy to silty texture and a highly variable boulder content. The till is classified as basal till on the basis of degree of compaction, striated clasts, and clast fabric by Nielson and Graham (1985). In low lying areas, the till sheet is covered by brownish-grey glaciolacustrine silt and clay, whereas the topographically high areas are generally covered or encircled by littoral sand and gravel deposits. Nielson and Fedikow (1986) have discussed a glacial dispersion train about 1.5 km long near the Dot Lake area, on the basis of arsenic concentration in the clay-size fraction and gold concentration in the heavy mineral fraction of the basal till. A similar dispersion train associated with the MacLellan (Agassiz) gold-silver deposit was noted to be only 150 m long. The difference in the lengths of these two dispersion trains has been attributed to the distinct outcrop patterns of mineralization with respect to the local topography. Nielson and Graham (1985) stated that in the Farley Lake area, there are no distinctive glacial dispersion trains associated with gold anomalies. They attribute the lack of evidence of glacial dispersal to the short distance of dispersion and a relatively large sample spacing.

### DATA EVALUATION

In any actively explored mining area there are often abundant detailed data available from the past and present exploration programs. A number of geological,

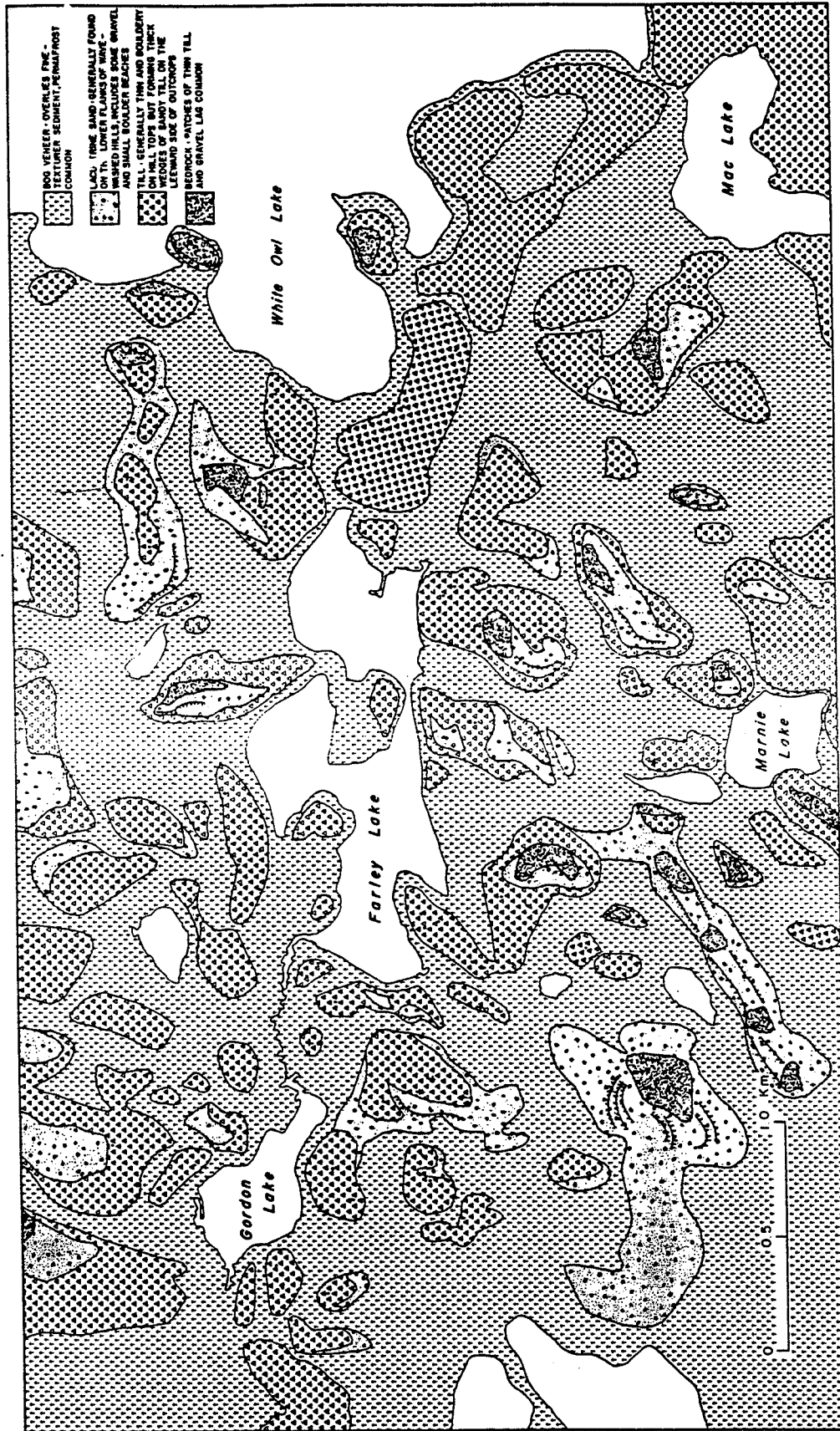


Figure 4. Surficial geology of the Farley Lake area, Manitoba (after Nielson and Graham, 1985).

geochemical, biogeochemical, and geophysical data sets are available for the Farley Lake area and its surrounding regions. Some of the data were initially acquired from various agencies for this study by Kettler and Anderson (1986).

A successful exploration program for any area requires review and reexamination of all possible data sets available. In this study a plan was initially made to integrate different types of data, and non-spectral ground based data have been gathered in support of, and as 'ground truth' for, the analysis of airborne spectral remote sensing data. In the following section the types of data available for the Farley Lake area are briefly reviewed and their usefulness for this study is discussed. The airborne multi-detector electro-optical imaging sensor (MEIS-II) data comprise the primary spectral remote sensing data, which is discussed in detail.

### Geological Data

The bedrock geology of the Farley Lake area (Figure 2) was mapped in detail by Gilbert et al. (1980); whereas the surficial geology of the area (Figure 4) has been described by Nielson and Graham (1985). Geological studies of the area surrounding Farley Lake and some of the producing deposits in the Agassiz Metallotect have been documented in detail in many of the Open File Reports of the Manitoba Energy and Mines.

### Geochemical Data

The analyses of till geochemical anomalies has proven to be successful for exploration of mineral deposits in many areas (Shilts, 1975, 1977, and 1984; Gleeson and Cormier, 1971; Garrett, 1971; and DiLabio et al., 1982). Till geochemistry provides a quick and economic means for identification of dispersion fans and trains in areas which are covered by glacial overburden. The dispersion fans and trains are produced down ice from the outcrops or subcrops, and mapping of these anomalies may lead to the identification of mineral deposits.

Promising areas in the Agassiz Metallotect have been sampled for detailed till geochemical studies, and a few dispersion trains have been recognized, particularly at the MacLellan gold-silver deposit and at the Dot Lake area (Nielson and Fedikow, 1986). Preliminary results of the till petrography and till geochemical studies at the Farley Lake were presented by Nielson and Graham (1985). Figure 5 shows the location of till samples. A total of 244 samples were collected from 216 holes and analysed by the Manitoba Geological Services under the supervision of E. Nielson. In the Farley Lake area, a distinctive glacial dispersion train has not been recognized; this is probably because the till represents the local component, or it may be due to the relatively large sample spacing compared to the size of the anomalies.

Nielson and Graham (1985) analyzed the basal till samples geochemically, and the data provided by them have been used in this study. They analyzed the clay-sized fraction, which consists of particles less than 1 microns in size, and the heavy mineral fraction, for each till sample. Cu, Pb, Zn, Ni, Co, Cr, Fe and Mn in both fractions were analyzed by atomic absorption spectrometry after hot nitric-hydrochloric acid extraction. Arsenic in both sets of samples was analyzed colorimetrically after nitric-perchloric acid digestion. The Au As analyses were not used in this study, because the data are semiquantitative, and were commonly expressed as "less than" ppb or ppm according to Nielson and Graham (1985).

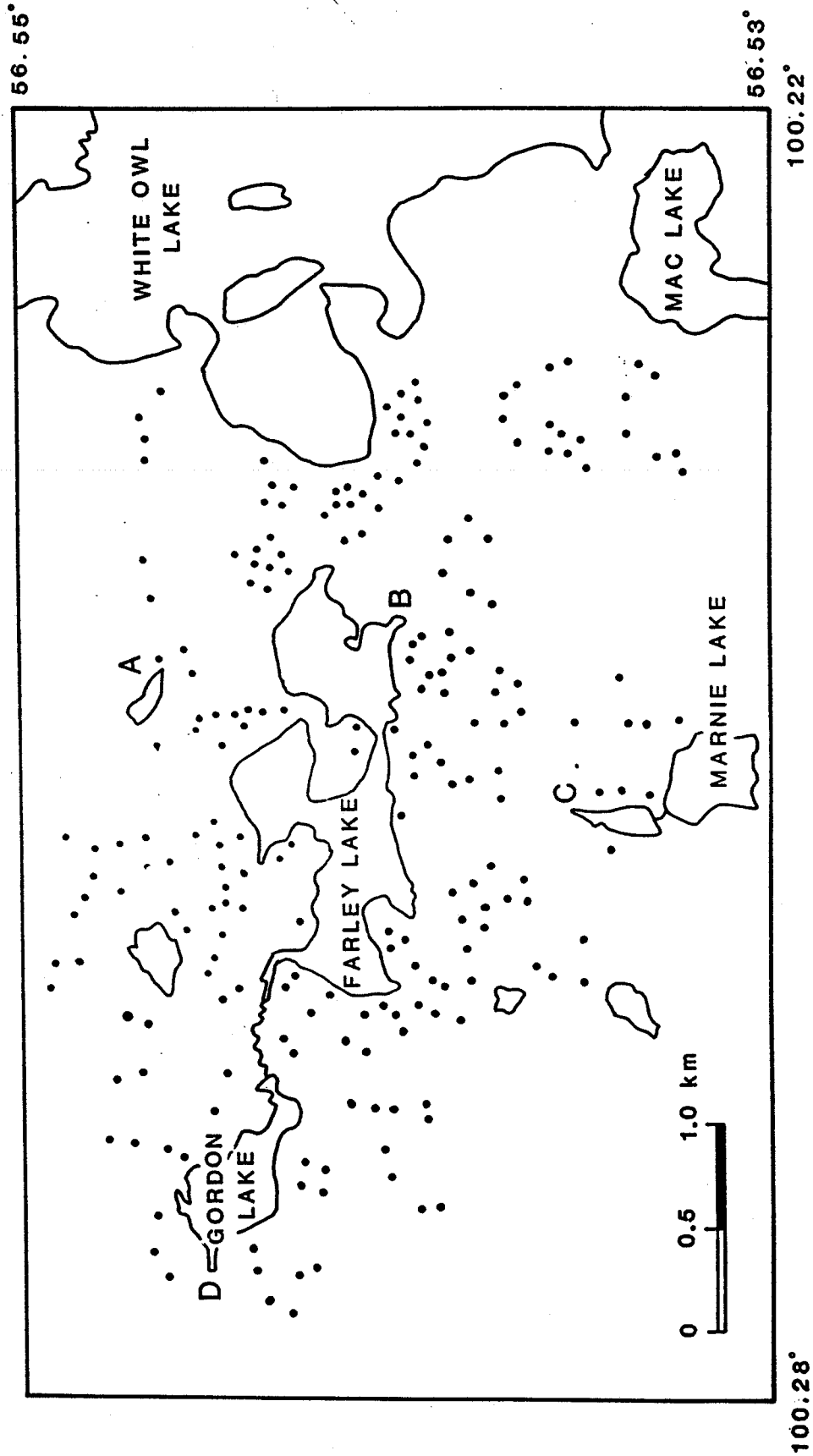


Figure 5. Location of till geochemical sample sites.

## Biogeochemical Data

Biogeochemical exploration methods have proven to be successful in many areas. This is because the plants growing on anomalously metal rich soils tend to have higher concentrations of those elements, and therefore anomalies in the soil and bed rock can be determined by sampling plant materials. Extensive geogeochemical sampling was conducted in the Agassiz Metallotect region by the Manitoba Geological Services under the supervision of M.A.F. Fedikow. The plant species sampled include black spruce (*Picea marina*) and labrador tea (*Ledum groenlandicum*); the needles, twigs, and bark samples were analyzed for trace element concentrations. Fedikow (1984, 1985) reported the results of the studies conducted around Dot Lake, Arbour Lake and the MacLellan gold-silver deposit. It was concluded that the biogeochemical anomalies provide cost effective and viable means of exploration for the Agassiz type strata-bound deposits. This is because plant organs tend to concentrate specific suites of elements. Black spruce as a sampling media is more acceptable than the labrador tea; the trace element contents of the black spruce reasonably approximate that of the underlying substrata. Some peat bog samples have also been analysed for the same area.

Orientation surveys originally conducted in the above areas were later extended to include the Farley Lake area. Nielson and Graham (1985) stated that there was some concern that the biogeochemical samples around the MacLellan gold-silver deposit might have been contaminated by airborne detritus from the mine tailings located about 7 km south at Lynn Lake. The Farley Lake area is located farther to the east, and sampling was extended around this area in order to duplicate the original multi-media geochemical study carried out around the MacLellan deposit.

Figure 6 shows the location of sampling grids in the Farley Lake area. At grid locations 1 through 3 black spruce needle samples were collected, whereas peat bog samples were collected at all five grid locations. Peat bog samples were analysed for Au and As concentrations, and black spruce needles for Cr, Cu, Zn, Ni, Mn, and Fe. All the elemental concentrations for the black spruce needles are expressed in ppm except for Mn, which is in percent. In this study black spruce needle sample analyses have been used. Peat bog samples at present are of limited use, because it is difficult to determine how much of the Au gold and As was initially accumulated in plants, and how much the Au gold and As concentrations were affected due to the mobility of elements after the plants were deposited as peat. However, some trace element anomalies in peat bogs may be related to trace elements of other concentrations in black spruce needles, but in order to interpret the geological significance of such anomalies detailed knowledge of ionic mobility and hydrogeochemistry would be necessary. Furthermore, the relationship of the elemental concentrations in the peat bog samples to the airborne spectral reflectance data would be fairly complex.

## GEOPHYSICAL DATA

### Airborne Electromagnetic Data

Much of the early interest in the Lynn Lake region stems from the EM INPUT surveys conducted by Questar Surveys Ltd. in 1976. The electromagnetic anomalies present in the region have been used to define the extent of the Agassiz Metallotect. This data set is available on a photo-mosaic base with electromagnetic anomalies registered to the appropriate locations. Due to the analog nature of this data set, it is not used in this study.

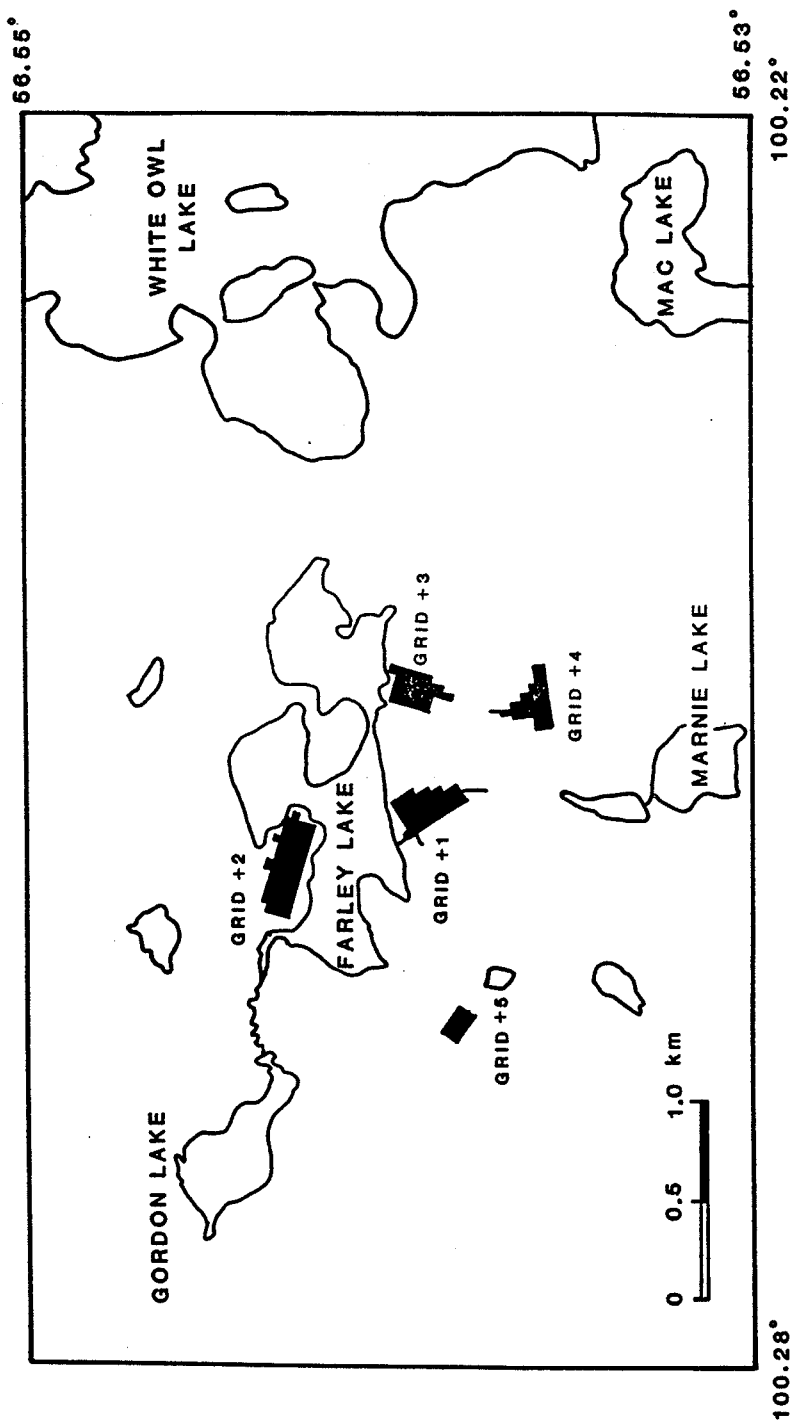


Figure 6. Location biogeochemical sample grids.

## **Aeromagnetic Data**

Vertical field gradiometric surveys have been conducted in the Lynn Lake region by the Geological Survey of Canada. Anomalous zones recognized from the aeromagnetic survey helped to delineate the Agassiz Metallotect (Figure 3). This data set is available in digital format on computer tapes. It consists of gamma values, and X and Y coordinates of the fiducial point location along the flight lines. Unfortunately, the fiducial point location is not provided properly; therefore it is difficult to determine the origin of the data set.

Any type of integration effort of this aeromagnetic data would require a correct geometrical registration and areal interpolation. However, the extensive interpolation of data, particularly when flight lines are spaced far apart tends to introduce smoothing effects, thereby reducing the high frequency components. The high frequency components are of a local nature and thus important for detailed analysis. Therefore, it is believed that the available aeromagnetic data can at best be used for regional scale study only.

## **Spectral Remote Sensing Data**

### *Landsat Imagery*

A Landsat computer compatible tape (CCT) covering the UTM sheet 64C with MSS bands 4 through 7 is available for the Lynn Lake region. In this case the pixel size is 79 x 79 metres and it does not have sufficient spatial resolution for detailed analysis; for this reason it has not been used in this study. Table 1 gives the spectral windows available for different bands in the Landsat MSS and Landsat TM data along with the dimensions of the spatial resolution cell.

### *Airborne Multispectral Data*

The airborne multispectral data, MEIS-II and MSS for the Lynn Lake region were collected by the Canada Centre for Remote Sensing (CCRS), with overflights on June 21, August 22 and 23, 1986. The purpose of the flights on two separate dates was to provide the temporal coverage for the Farley Lake area. The sensors were flown at two different altitudes. The high altitude flight was to provide a low resolution region coverage, whereas the low altitude flight was to provide detailed coverage of high spatial resolution. The data sets for the MEIS-II and MSS are in the digital format and are available in CCT format. The different dates, altitudes, and image centres as obtained from the computer printouts accompanying the data are listed in Table 2. Some of the image centres are approximate and to determine the precise location of the image, it was displayed on the screen and compared with the topographic map of the area. Spectral windows used for data acquisition are listed in Table 1. Unfortunately, due to navigational error, all of the high altitude flights are outside of the study area (Farley Lake area), and only the low altitude flight lines of June 21, 1986 provide the coverage for the area of this research. However, as mentioned earlier, these data sets are available on CCTs and may be of use in future, when more detailed work is done in the areas surrounding the Farley Lake. In this study only the low altitude flight data of June 21, 1986 has been used for the purpose of analysis.



**Table 1. Comparison of Landsat MSS and TM system configuration**

**Landsat system characteristics**

Multispectral Scanner (MSS)		Thematic Mapper (TM)	
Band number	micrometers	Band number	micrometers
4	0.5-0.6	1	0.45-0.52
5	0.6-0.7	2	0.52-0.60
6	0.7-0.8	3	0.63-0.69
7	0.8-1.1	4	0.76-0.90
		5	1.55-1.75
		7	2.08-2.35
		6	10.40-12.5
spatial resolution: 79 x 79 meters		30 x 30 meters for band 1-5, 7 120 x 120 meters for band 6	

**Spectral Reflectance Properties of Vegetation**

The information regarding the spectral reflectance properties of vegetation have been reported by a number of investigators (Colwell, 1974; Gausman, 1977; Tucker, 1980; Smith, 1983; Goetz et al., 1983; Horler et al., 1983; Chang and Collins, 1983; Westman and Price, 1988), some of which are not referenced individually. A typical spectral reflectance curve for an actively photosynthetic plant leaf obtained using a portable field spectrometer is shown in Figure 7. The general optical properties of leaves and underlying mechanisms are fairly well understood. The low reflectance and transmittance in the visible portion of the electromagnetic spectrum is attributed to chlorophyll absorption and other pigments at the blue and red wave lengths. The weak reflectance feature at 0.52 and 0.60  $\mu\text{m}$  indicates the portion which is not strongly absorbed, resulting in the green appearance of plant leaves to the human eye. The sharp rise in the curve between the chlorophyll absorption feature at 0.68  $\mu\text{m}$  and the near-infrared plateau is referred to as the red edge, and the slope of the red edge has been related to chlorophyll concentrations in the leaf (Holser et al., 1983). In the near-infrared region (0.75  $\mu\text{m}$  to 1.35  $\mu\text{m}$ ), because of the leaf's internal cell structure, multiple scattering occurs and reflectance and transmittance tends to be in the 40 to 50 percent range. Strong water absorption bands occur in the middle infrared region up to 2.0  $\mu\text{m}$  with specific water absorption bands centred at roughly 1.4 and 1.9  $\mu\text{m}$ . There is a considerable difference in leaf reflectance according to the leaf-type, particularly in the near-infrared region.

The spectral curve of leaves generally changes during the growing season, which in turn reflects change in chlorophyll concentrations as well as build up of additional pigments within the leaves. As the leaves mature, their visible reflectance tends to decrease, while the near-infrared reflectance increases. Moreover, both the position and slope of the red edge changes during the gradual change in the leaves from active photosynthesis to total senescence. The optical behavior of leaves is also affected by the various types of stress, as well as nutrients, salinity and geobotanical environmental conditions. The top and bottom surfaces of a leaf may exhibit differences in reflectance and transmittance properties. This type of information is most important, particularly when detecting stress in vegetation for

**Table 2. System characteristics for airborne data collected for the Lynn Lake region for this study.**

Band number	Center (nm)	Band width (nm)
<b>MEIS-II 8 Channel data of June 21, 1986 and August 23, 1986</b>		
1	776.31	36.84
2	675.33	38.74
3	746.75	16.77
4	480.82	31.40
5	734.33	16.98
6	710.22	15.52
7	698.34	13.09
8	548.56	31.60
Spatial resolution: 6.3 x 1.9 metres		
<b>MSS 10 Channel data of August 21, 1986</b>		
1	432.50	35.00
2	470.00	50.00
3	525.00	50.00
4	572.50	45.00
5	617.50	55.00
6	660.00	70.00
7	730.00	100.00
8	830.00	130.00
9	950.00	170.00
10	visible range	
Spatial resolution: 9.9 x 3.5 metres		
<b>MSS 5 Channel data of August 23, 1986</b>		
1	470.00	50.00
2	572.50	45.00
3	60.00	70.00
5	visible range	130.00
Spatial resolution: 6.1 x 2.0 metres		

geobotanical investigations. Other factors which affect reflectance of leaves include moisture content, orientation, and stacking of leaf layers as discussed by Westman and Price (1988).

The spectral properties of leaves also vary to a large extent depending on the season and the type of vegetation involved. For example, the deciduous trees show variation in chlorophyll contents and the density of leaves in different seasons. In contrast to deciduous trees, conifer trees always contain a large amount of chlorophyll; however, the young leaves tend to be brighter, because the chlorophyll absorption bands for collection of conifer leaves are subdued early in the growing season. Also there is no period when all the leaves die, so there is no drastic change in reflectance throughout the year.

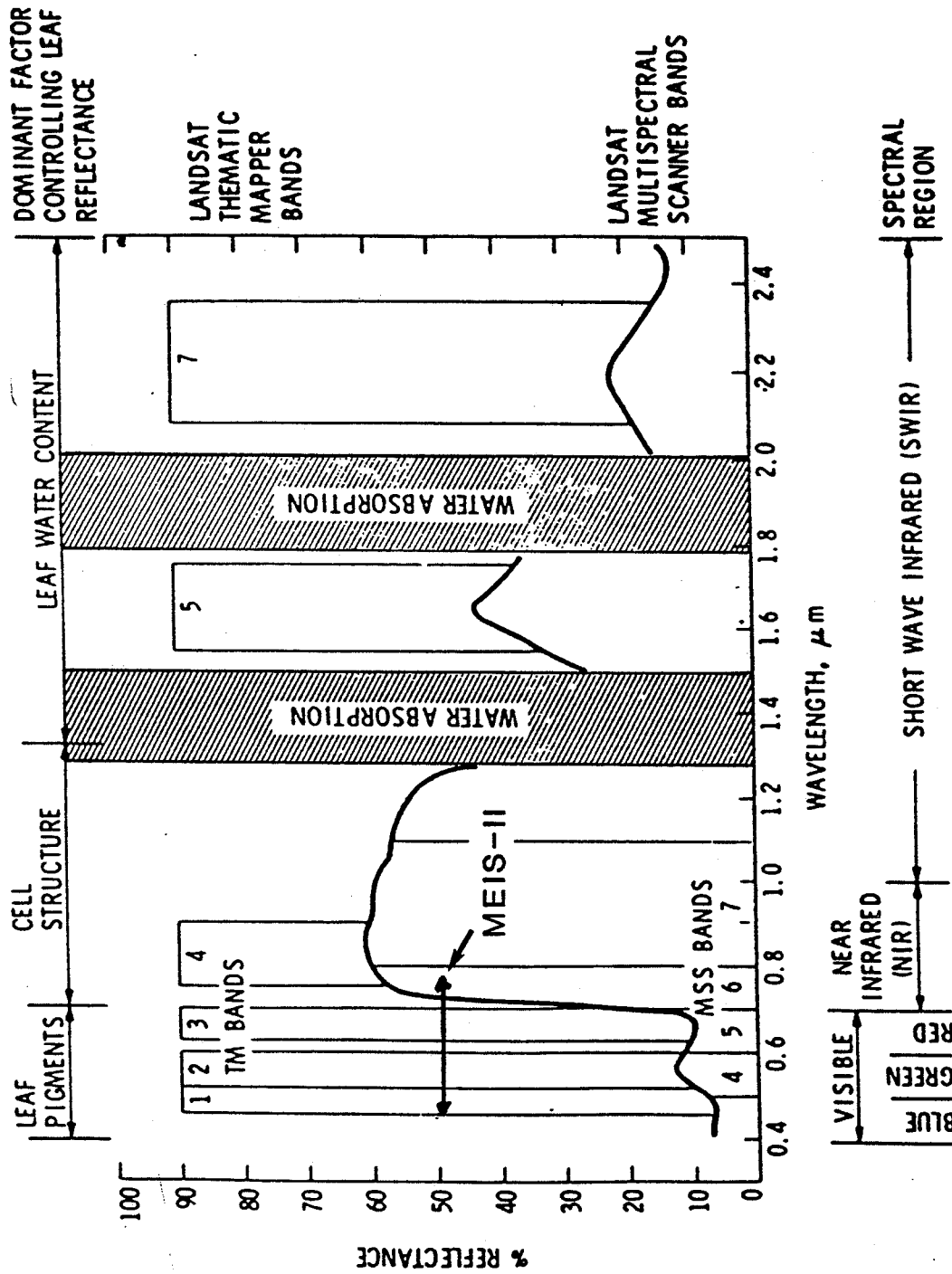


Figure 7. Typical spectral reflectance response of a plant leaf as obtained by a portable field spectrometer (after Goetz et al., 1983).

## Reflectance Properties of Vegetation Canopy

A plant is a collection of leaves and numerous voids between leaves. Electromagnetic waves are reflected, absorbed, emitted, and transmitted by leaves, and this radiation may be re-reflected numerous times before leaving the plant. The spectral reflectance properties of plants are much more variable and complex than that of leaves. This is because a number of other parameters affect the reflectance properties of plants, some of which include, number and arrangement of leaves; spectral characteristics of trunk and stalks; reflectance properties of the background, that is, soils, rocks, and understory shrubs and vegetation litter; the solar zenith and the look direction. These reflectance properties may exhibit local maxima and minima, but are highly variable.

In this study the MEIS-II data of June 21, 1986 and MSS data of August 23, 1986 flights have been used. The spatial resolution for the MEIS-II data pixel size is  $6.3 \times 1.9$  metres, whereas the MSS data pixel size is  $6.1 \times 2.0$  metres. Due to the wide spectral windows in most of the bands only band 1 and band 2 have been used for the purpose of correlation with the geochemical and biogeochemical data. MEIS-II data provides a reasonable coverage for the area of this research, whereas the MSS data passes through the northern part of the area, and covers only the biogeochemical grid location number 2. Furthermore, when the MSS data are displayed on the screen, each image is somewhat fuzzy, which may be due to defocusing during data collection, or may be due to random noise of the system.

## DATA ANALYSIS

The data analysis approach applicable to any geological situation depends on the type of data available and to some extent on the nature of the problem under consideration. Whenever multi-media data sets are available for a particular area, there is an attempt to integrate these different types of data for a meaningful relationship to extract information, rather than to try to estimate each type of parameter separately as represented by each data set. The data can be grouped in three broad types, irrespective of its sampling media, that is, whether geophysical, geochemical, or biogeochemical:

1. **Sequential Data:** this type of data is characterized by their position along a line; for example aeromagnetic data consist of magnetic field values which are measured along a flight line and the flight lines may be running across the anomalous zone. The chemical analysis of till data obtained at certain depth intervals is also a sequential type data.
2. **Map Data:** an extension of the sequential data in two-dimensions represents map data. In this situation, a particular variable is measured as a function of its geographic location, which is represented in terms of an X and Y coordinate system. Map data represent a continuous function in two-dimensions based on the discrete observations at control points (Davis, 1973). The concentrations of each element in the till geochemical and biogeochemical data sets represent map data, as the variations in concentrations of each element can be displayed in terms of a map. Similarly, the multispectral reflectance data for an individual band are also two-dimensional map data. In this situation the digital number at each pixel is characterized by its geographic location.
3. **Multivariate Data:** In multivariate data, each observation is characterized by several variables; that is changes in several properties are considered simultaneously at each observation point. The geochemical and biogeochemical data with all the elements considered at the same time represent multivariate

data sets. Similarly, when all the bands of the multispectral data for MEIS-II and MSS are considered, they also constitute multivariate data sets.

All the three types of data are available for the Farley Lake area, and for the purpose of integration, the data have been processed by keeping in view the following objectives:

1. Data rectification: it generally involves the compensation or correction of data for geometric and/or radiometric distortions. Sometimes transformation of the data set may be necessary.
2. Data reduction: it is carried out by using certain statistical parameters to eliminate redundancy in the data, so that the meaningful relationships can be presented for a suitable display and interpretation.
3. Interpolation: when the original data are sparse, several values must be estimated for each pair of observations. If there are many more original points than the interpolated points, in that situation some of the original data points are ignored because the surrounding values determine the interpolated values. The estimation of data between the known points can be accomplished by averaging.
4. Data display: this involves the display of different data sets or their relationships to a uniform scale, so that meaningful information can be extracted. The map data may be processed before displaying to enhance certain features of interest.

A general flow chart showing the data processing scheme for the Farley lake area is shown in Figure 8. The following section describes some of the processing steps in detail.

#### *Biogeochemical and Geochemical Data*

The biogeochemical and till geochemical data were obtained as maps displaying sample locations and hard copies of tables showing concentration of elements at each sample location. In order to process this data and integrate it with other types of data, it must be in digital format so that it can be digitally manipulated. The sample locations in biogeochemical and geochemical maps were digitized by assigning X, Y coordinates to each sample location so that it can be easily identified, and then by inputting the corresponding elemental concentrations. The X, Y coordinate system is an arbitrary system depending on the location of the origin; in order to compare the multi-media samples the observations must be made with respect to the common location of the origin in different data sets. To facilitate the comparison of geochemical and biogeochemical data sets, longitude and latitude values were computed from the X and Y coordinate system. Unfortunately, only two of the till geochemical samples are located in the area corresponding to the location of the biogeochemical grid 2, and all other samples are located outside the grid boundaries of the biogeochemical grids (Figure 5 and 6). This makes the comparison of the biogeochemical data with the till geochemical data at the corresponding or even at a nearby location almost impossible. However, the two data sets were compared with the airborne multispectral remote sensing data.

For the biogeochemical data, equally spaced grid nodes were computed corresponding to three grid locations for each element in the data set. These grids were used to produce two-dimensional maps to identify the biogeochemical anomalies.

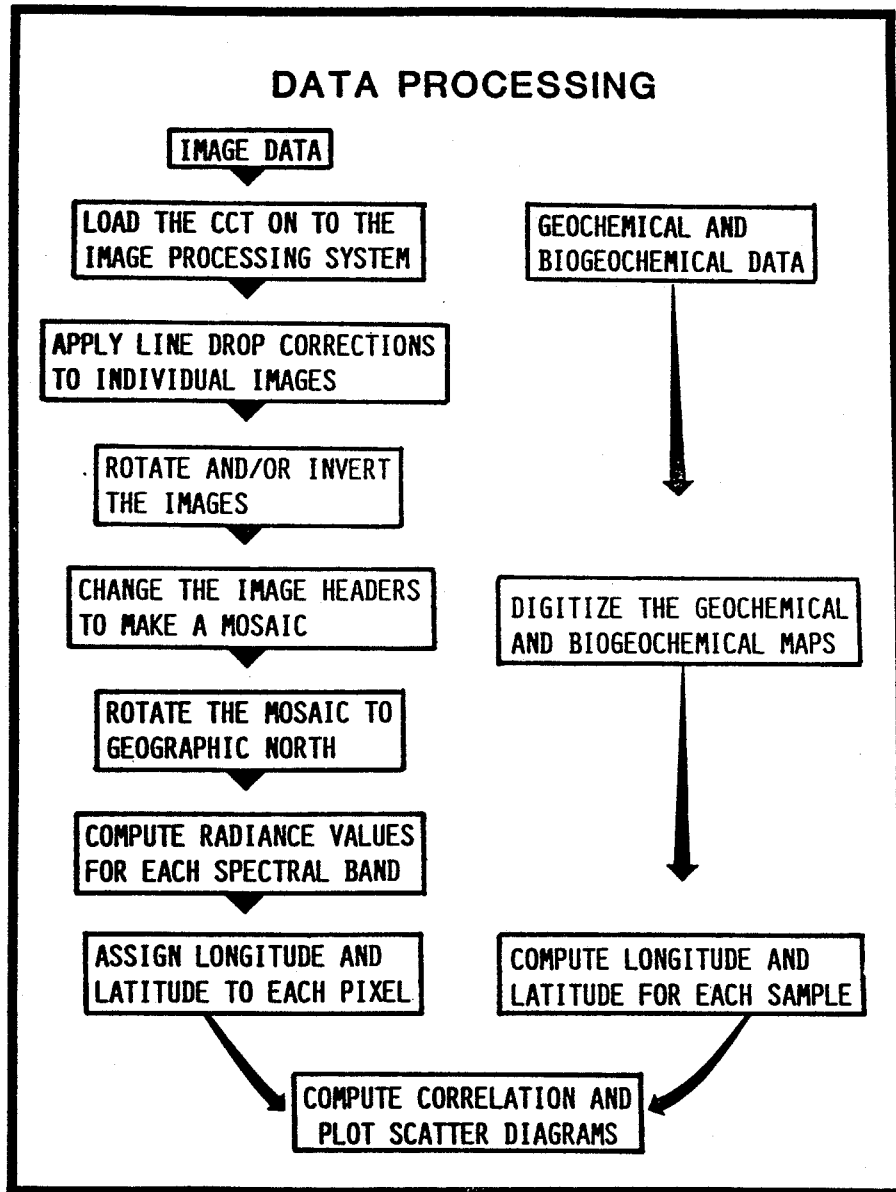


Figure 8. Data processing flow chart.

### *Multispectral Remote Sensing Data*

To process the multispectral remote sensing MEIS-II and MSS data of the Farley Lake area, the following steps were used:

1. **Reading of the CCTs:** The airborne MEIS-II and MSS data are provided by the CCRS on computer compatible tapes (CCTs). The data obtained for the Farley Lake area are in raw form and have band interleaved by line (BIL) organization. To read the CCTs, certain parameters, such as the number of lines, number of pixels, scan line offset and the scan line fill were determined. These parameters are different for each of the MEIS-II and MSS tapes. By knowing these parameters a format file was created, which facilitates the reading of CCTs onto the Image Processing System. Once the CCTs were read in, images were displayed to identify their locations by comparing them to the topographic map. Some of the images had to be rotated and inverted, because the top of the image was pointing in the flight direction.
2. **Line Drop Correction:** The most common type of radiometric distortion in the MEIS-II and MSS data are the line drop distortions. This means that a particular scan line does not match the adjacent lines. The dropped line is either too bright or too dark, thereby indicating a detector malfunction and this gives the image a striped appearance. The line drop correction can be applied by replacing the distorted line either by the immediate top or the bottom line, or by the average of the two. Usually the average of the immediate adjacent lines is more acceptable, because the image reflectance values can be considered as spatially continuous.
3. **Area of overlap:** Once the images have been radiometrically corrected, the next step is to determine the area of overlap in adjacent images, that is along the flight and between the flights. This was carried out by displaying two adjacent images in correct spatial position and identifying the same geographic features on both images. In the absence of recognizable geographic features, patterns in the pixel intensities in two adjacent images were used. As the images are recorded in terms of number of lines and number of pixels, the area of overlap can be expressed in terms of lines and pixels.
4. **Header modification:** Image headers contain information such as start line, start pixel, number of lines, number of pixels, minimum, maximum, mean and standard deviations of the pixel values for that particular band. Once the area of overlap was determined, the image headers were modified so that the different images occupied the correct spatial position. Image headers had to be modified separately for each of the bands involved.
5. **Mosaic Construction:** After the image headers had been modified, different images for the same spectral band were combined to make a mosaic. Figure 9 shows the different images used to make a mosaic, and the mosaic of band 1 of the MEIS-II data for the Farley Lake area is shown in Figure 10. Mosaics of different spectral bands tend to show some geometrical distortions. The distortions may be due to offset, which is the shift of pixels. This was corrected geometrically by image to image registration. The procedure involves identifying a series of ground control points on the master image in terms of pixel location, and identifying the same points on the slave image. This correspondence between locations on the two maps is used to generate an algorithm that will resample the slave image into the same projection as the master image.

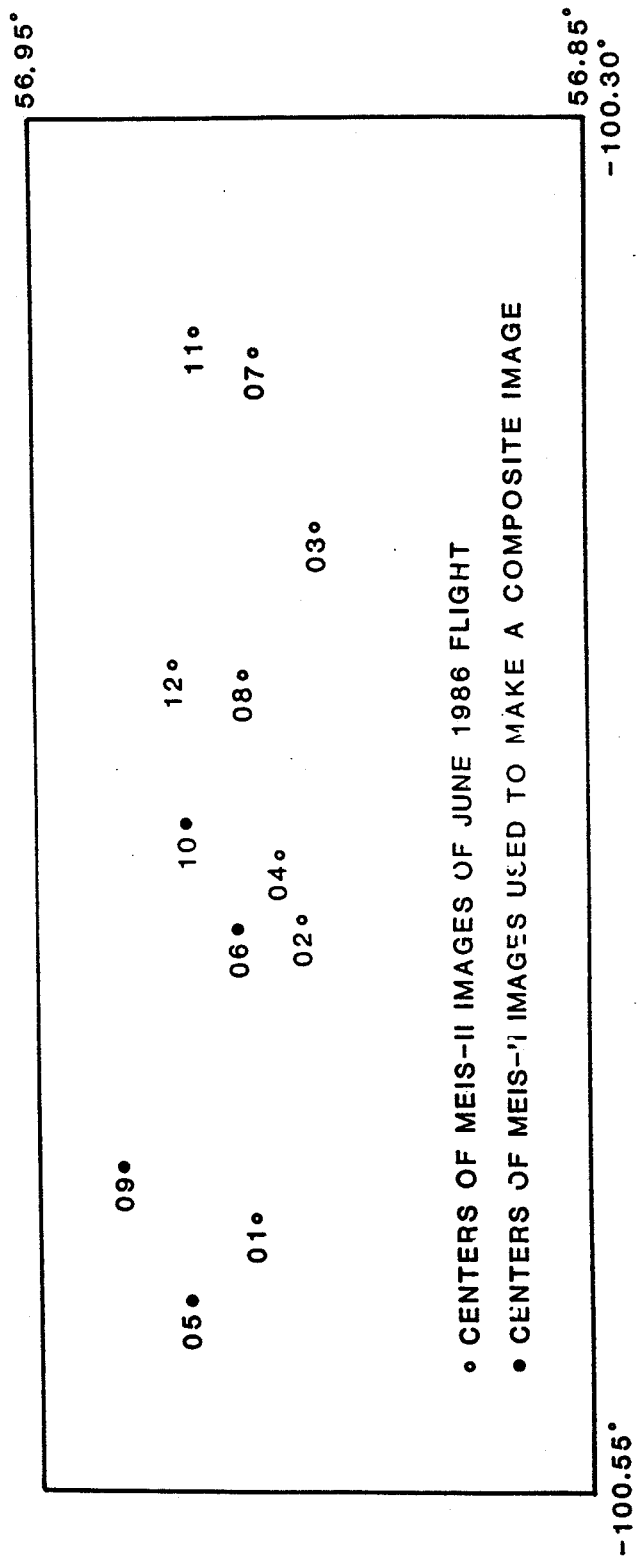


Figure 9. Location of MEIS-II image centers used for the construction of a mosaic.



6. **Rotation of mosaic:** The mosaic image is oriented in the direction of flight line. By comparing the mosaic with the topographic map, angle of rotation was determined, and the mosaic was rotated accordingly so that the top of the mosaic was oriented to the geographic north. Because the original mosaic was produced from a combination of four separate images, the size was often large, as it had more than a few million pixels. Such large images are difficult to manipulate, and therefore it was resampled to reduce the number of pixels using the nearest neighbour averaging method.
7. **Assign coordinates to pixels:** The image is a matrix of numbers, and an individual pixel in the image is identified by line and pixel number. In order to compare this image with other types of map data, the pixels must be identified by their location in terms of a coordinate system. By knowing the line and pixel number, pixels were assigned X, Y coordinates. Then, from the topographic map, longitude and latitude for known geographic features were determined, and longitude and latitude of the pixels were computed.

### *Hardware Requirements*

Each MEIS-II and MSS image contains about 1024 pixels and about 4000 lines, which is equal to about  $4.096 \times 10^6$  pixels. A mosaic produced by a combination of four such images (as in this study) would have more than 16 million pixels. A pixel is one byte long; a mosaic of this size would occupy more than 16 megabyte of disk storage. For the computation purposes, the pixel is converted to an integer number which is two byte long, and then to a real number (floating point number), which is four bytes long. When each of these pixels are assigned X and Y coordinates, they take up enormous amounts of disk space. These types of computations can only be carried out with a medium to large computer system, with large disk space and enough memory.

### *Correlation of Data Sets*

Once the longitude and latitude values have been assigned to various samples in different data sets, they can be compared and their relationships can be determined. A number of techniques are available for the integration of data sets; these include the simple technique of correlation analysis to mathematically more rigorous techniques of inversion of data sets (Towmey, 1977). Davis (1973) has discussed some of the techniques for comparing two-dimensional map data, whereas techniques used for multivariate data have been discussed by Sokal and Sneath (1963); Cooley and Lohnes (1971); and Morrison (1973). Integration techniques, particularly involving remote sensing data and display methods, are given by Eliason et al. (1983) and by Guinness et al. (1983).

In this study different types of data have been correlated by calculating the Pearson-product moment correlation coefficient, which is expressed as:

$$r_{jk} = \frac{\sum_{i=1}^n X_{ij} X_{ik} - \left( \sum_{i=1}^n X_{ij} \sum_{i=1}^n X_{ik} \right) / n}{\left\{ \sum_{i=1}^n X_{ij}^2 - \left[ \left( \sum_{i=1}^n X_{ij} \right)^2 / n \right] \right\} \left\{ \sum_{i=1}^n X_{ik}^2 - \left[ \left( \sum_{i=1}^n X_{ik} \right)^2 / n \right] \right\}}$$

where  $r_{jk}$  is correlation coefficient between two variables  $X_{ij}$  and  $X_{ik}$  and  $n$  is the number of data points. The correlation coefficient,  $r$  varies between +1.0 to -1.0; a positive value of  $r$  indicates that the variables are directly related, whereas a negative value implies an inverse relationship. The values of  $r$  which approach +1.0 or -1.0 represent a linear relationship, and values close to zero indicate lack of linear relationship between the two set of variables. The results of linear correlation analysis are only significant when data have a normal distribution. In this study the data were not statistically checked for the normal or any other identifiable distribution. However, the frequency distribution diagrams given by Nielson and Graham (1985) for till geochemical data for the Farley Lake area appear to have a more or less normal distribution. Fedikow (1985) shows the frequency distribution for biogeochemical data from the Agassiz stratabound Au-Ag deposit; these data also appear to have a normal distribution. The linear correlation between different pairs of variables have been calculated and are shown as a correlation matrix (Tables 3 to 5), for each of the biogeochemical grid locations and airborne data. Tables 6 and 7 show the linear correlation between different pairs of geochemical data and multispectral airborne data.

**Table 3.** Correlation matrix of biogeochemical data from grid 1 and MEIS-II spectral data for the Farley Lake area.

	Ash	Cr	Cu	Ni	Zn	Mn	Fe	Bnd 2	Bnd 1
Ash	1.0								
Cr	-0.0481	1.0							
Cu	-0.7840	0.0185	1.0						
Ni	-0.6307	0.1075	0.5034	1.0					
Zn	-0.2259	-0.0303	0.0414	0.2283	1.0				
Mn	-0.5861	0.0199	0.5066	0.5766	0.2912	1.0			
Fe	-0.4046	0.1689	0.4018	0.2435	0.1969	0.1369	1.0		
Bnd 2	0.1237	0.1041	0.0675	-0.1360	-0.2725	0.0549	0.1667	1.0	
Bnd 1	0.0518	-0.1393	0.0855	-0.1194	0.1558	0.0517	0.1010	0.2664	1.0

The relationship between two variables can be conveniently displayed as bivariate scatter plots. The scatter plots show the distribution of data, and if there is a poor correlation, the distribution of points is fairly random (Figure 10).

## INTERPRETATION

In this study correlation between different types of data namely, airborne multispectral, geochemical and biogeochemical data have been estimated for the Farley Lake area. The results are presented in the form of correlation matrices.

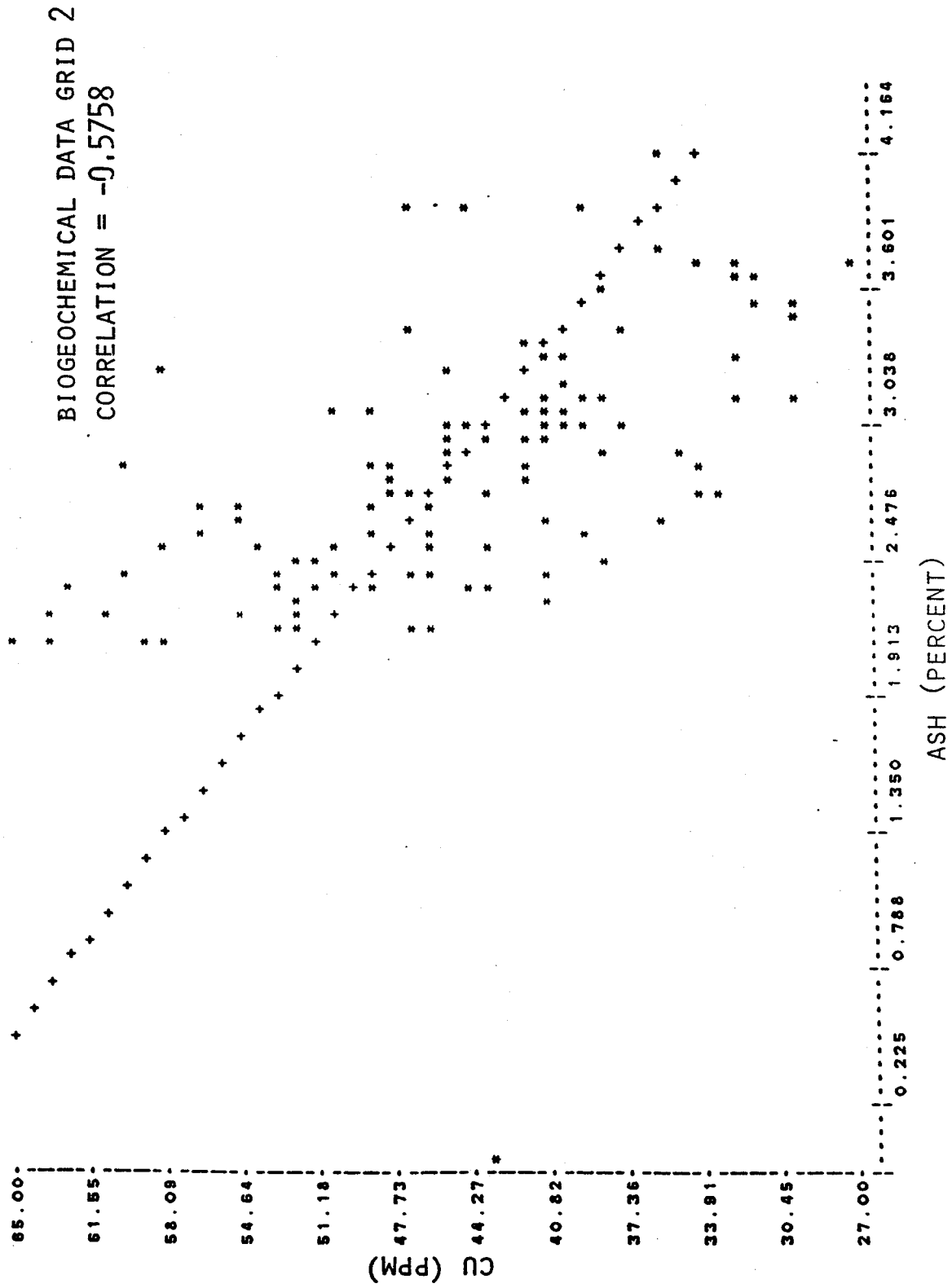


Figure 10. Scatter plot of the biogeochemical data from grid 2 showing concentration of copper versus ash concentration.

**Table 4. Correlation matrix of biogeochemical data from grid 2 and MEIS-II and MSS spectral data for the Farley Lake area.**

	Ash	Cr	Cu	Ni	Zn	Mn	Fe	Bnd 2	Bnd 1	Mss2	Mss1
Ash	1.0										
Cr	-0.1211	1.0									
Cu	-0.5758	0.0989	1.0								
Ni	-0.0862	0.2004	0.0821	1.0							
Zn	0.1170	0.0227	-0.0942	0.2710	1.0						
Mn	-0.1935	-0.1093	0.1189	-0.0763	0.2002	1.0					
Fe	-0.3503	0.4096	0.3039	0.4056	0.0766	0.0772	1.0				
Bnd 2	-0.0060	0.0736	-0.036	0.0743	-0.0478	-0.1543	0.0381	1.0			
Bnd 1	-0.0612	0.0965	0.0157	0.1020	0.0176	-0.0810	0.1299	0.6938	1.0		
Mss 2	0.0752	0.0884	-0.1618	0.0447	-0.1162	-0.0526	0.0682	-0.0365	-0.0366	1.0	
Mss 1	-0.0962	-0.0715	0.1153	0.0918	0.0326	0.1292	0.3362	-0.0506	0.0063	0.0825	1.0

**Table 5. Correlation matrix of biogeochemical data from grid 3 and MEIS-II spectral data for the Farley Lake area.**

	Ash	Cr	Cu	Ni	Zn	Mn	Fe	Bnd 2	Bnd 1
Ash	1.0								
Cr	-0.0724	1.0							
Cu	-0.0897	0.0847	1.0						
Ni	-0.1464	0.1169	0.3406	1.0					
Zn	0.4619	-0.0222	0.1845	-0.0813	1.0				
Mn	0.0875	0.2055	0.5529	0.3655	0.1436	1.0			
Fe	-0.1350	-0.0563	0.4866	0.4522	0.2035	0.2615	1.0		
Bnd 2	-0.2604	0.0027	0.3463	0.3011	0.0226	0.0137	0.5097	1.0	
Bnd 1	-0.1247	-0.0858	0.3400	0.2405	0.0085	-0.0291	0.2414	0.6614	1.0

**Table 6. Correlation matrix of clay-sized fraction of till geochemical and MEIS-II multispectral data for the Farley Lake area.**

	Cu	Pb	Zn	Co	Ni	Cr	Mn	Fe	As	Bnd 2	Bnd 1
Cu	1.0										
Pb	-0.0204	1.0									
Zn	0.1334	0.1487	1.0								
Co	0.0130	0.0059	0.1409	1.0							
Ni	0.2564	0.0481	0.4719	0.2800	1.0						
Cr	0.0493	-0.0716	0.4345	0.3694	0.4093	1.0					
Mn	0.2343	0.0305	0.5199	0.4780	0.3386	0.4312	1.0				
Fe	0.2187	0.1476	0.7361	0.3054	0.3881	0.7010	0.4737	1.0			
As	0.2334	0.0676	0.0471	0.0316	0.0830	-0.0061	-0.0394	0.0808	1.0		
Bnd 2	-0.0600	0.0112	-0.0790	0.0019	0.0204	-0.0902	-0.0752	-0.0948	-0.0280	1.0	
Bnd 1	0.0414	0.0173	-0.0335	-0.0076	-0.1174	-0.0749	-0.0153	-0.0134	-0.01748	0.0345	1.0

**Table 7. Correlation matrix of heavy mineral fraction of till geochemical data and MEIS-II multispectral data for the Farley Lake area.**

	Cu	Pb	Zn	Co	Ni	Cr	Mn	Fe	Bnd 2	Bnd 1
Cu	1.0									
Pb	-0.0831	1.0								
Zn	0.0265	0.0716	1.0							
Co	0.1033	-0.0057	0.5261	1.0						
Ni	0.0965	-0.2503	0.5250	0.4596	1.0					
Cr	0.0665	-0.2051	0.4733	0.4128	0.6886	1.0				
Mn	-0.1339	-0.4209	0.6976	0.4021	0.3186	0.3407	1.0			
Fe	-0.0875	0.3797	0.6224	0.4653	0.2731	0.2938	0.8335	1.0		
Bnd 2	0.0732	-0.0133	0.0327	-0.1111	-0.0296	-0.0331	-0.0469	-0.0872	1.0	
Bnd 1	0.1044	0.0729	-0.0396	-0.0683	-0.0809	-0.0183	-0.0474	-0.0330	0.0279	1.0

## **Biogeochemical Data**

The correlation matrices of the biogeochemical data and multispectral remote sensing data for grid number 1 through 3 are given in Tables 3 to 5.

### *Grid 1 Biogeochemical Data*

The ash content of black spruce for Grid 1 shows a strong inverse relationship with most of the elemental components. Chromium displays a lack of correlation with most of the other elements. The element copper, has a positive correlation with Ni, Mn, and Fe. Nickel displays a positive correlation with Mn, whereas the zinc appears to have no correlation with any other elements in this biogeochemical grid. Manganese has fairly good correlation with Cu and Ni; whereas, iron displays good correlation with Cu concentrations.

### *Grid 2 Biogeochemical Data*

The ash content displays negative correlation with most of the elements analyzed. Copper shows moderate relationship with Fe, whereas Ni has a positive correlation with Fe and in general iron and manganese do not indicate any significant relationship with most of the other elements. The multispectral remote sensing data, that is, the MEIS-II and MSS also do not appear to have any correlation with the biogeochemical distribution of elements in the samples.

### *Grid 3 Biogeochemical Data*

Copper concentrations in biogeochemical data have some correlation with Mn and Fe. Nickel also shows positive correlation with Fe and Mn. Manganese displays a good relationship with Cu and Ni, whereas the zinc displays a lack of correlation with most of the elements analyzed. In this case the band 2 of the MEIS-II data indicates a positive correlation with iron; whereas the band 1 and band 2 display moderate correlations with the copper concentration. However, the correlation between the MEIS-II and biogeochemical data should be interpreted with caution, because the grid 3 has a small number of samples as compared with the other biogeochemical grids.

The negative correlation between the ash content of the black spruce needles and the copper elemental concentrations can be displayed for interpretation purpose in the form of two-dimensional maps. However, this negative correlation appears to be probably due to the closed nature of the system, because the elemental analysis was performed on the plant ash material.

From the correlation matrices of the biogeochemical data, it is clear that some of the element pairs in different biogeochemical grids do not have the same degree of linear relationship. This makes the interpretation of the biogeochemical anomalies difficult. Brooks (1972, 1983) has enumerated a number of factors which affect the accumulation of different elements in the plants and thus the interpretation of the biogeochemical data. Some of these factors include: type of plant sampled, plant, depth of the root system, pH of the soil, drainage in the area, availability of elements, rainfall, variable shading, antagonism of other elements, and soil temperature. Any variation in these factors could affect the accumulation of elements in the plants, and some of these factors may have more pronounced effect than the others.

## Geochemical Data

Geochemical analysis of the basal till samples for the two data sets, the clay-sized fraction and heavy mineral fraction, have been interpreted.

### *Clay-sized Fraction*

The linear correlation among different elements in the clay-sized fraction of the till data are given in Table 6, and the following observations can be made.

The element copper shows poor correlation with other elements analyzed in the clay-sized fraction of the till samples. This may be due to high mobility of copper in acidic solution with pH below 5.5 (Hawkes and Webb, 1962). This type of acidic solution may exist in areas with decaying organic material. The fairly high average concentration of copper in the clay fraction could be attributed to its adsorption by clay minerals. Like copper, lead is a chalcophile element, and it also has low correlation with other elemental concentrations in the till samples. The element zinc, has a high linear correlation with Ni, Cr, Mn, and Fe. Zinc has moderately high mobility, but its mobility is limited by organic activity and coprecipitation with limonite (Hawkes and Webb, 1962). Cobalt, displays positive correlation with Cr, Fe, and Mn. Nickel in the clay-sized fraction of the till samples shows a positive correlation with Cr, and to some extent with Mn and Fe. Similarly chromium has a linear correlation with Mn and Fe. Manganese has fairly low mobility, and is positively correlated with Fe, Ni, Cr, and Zn. Iron in the clay-sized fraction of the till data also displays linear relationship with Cr, Mn, Co, Ni, and Zn. Arsenic does not have any significant correlation with any of the elements in the clay-sized fraction.

According to Horsnail and Elliott (1977), pronounced variations in Eh and pH are frequently encountered in areas with poorly drained soils and organic-rich surface horizons; this appears to be the situation in the Farley Lake area. Decomposition of plant materials render ground waters acidic and such ground waters can dissolve appreciable quantities of Fe, Mn, Ni, Co and Zn. When this acidic water mixed with the fresh water, the pH commonly rises, resulting in the precipitation of Fe and Mn. These freshly precipitated manganese hydroxides have negative charges and attract divalent cations. Generally, the hydroxides of Fe and Mn can act as a 'sink' for many of the heavy metals. These compounds commonly form thin coatings on mineral grains in soils and sediments, and thus exert an adsorptive influence on other cations.

The MEIS-II spectral bands, band 1 and band 2 lack any significant correlation with the elemental concentrations in the clay-sized fraction of the basal till data. In this situation, reflectance in any particular spectral window may not have any geochemical significance.

### *Heavy Mineral Fraction*

According to Nielson and Graham (1985), the non-magnetic heavy mineral fractions in the Farley Lake area include, opaque minerals (mainly ilmenite), hornblende, and epidote. These minerals constitute more than 60 percent of the heavy mineral fraction, and were derived from the underlying iron formation and the volcanic rocks around the Farley Lake area. The remaining heavy minerals were derived from multiple sources, north of the study area, and are indicators of provenance of the far travelled component of the till. These include, garnet, hypersthane, zircon, and sphene.

In the heavy mineral fraction, copper shows lack of significant correlation with any of the elements analysed. Lead has a somewhat positive correlation with iron, and manganese. The element zinc displays positive correlation with the ferrous elements, namely, Co, Ni, Cr, Mn and Fe; whereas the cobalt, has linear relationship with Ni, Cr, Mn, and Fe. Nickel has a strong relationship with Cr, and moderately positive relationship with Mn. Manganese has a strong relationship with Fe and Zn, and moderate relationship with Co, Ni, Cr, and Pb; whereas the iron has positive correlation with Mn, Zn, Co, and Pb, and weak correlation with Ni and Cr. This may be due to the fact that the iron formation provides the bulk of the heavy minerals and it is interbedded with characteristic high Mg-Ni-Cr basalt. The basalt (a volcanic rock) supplies the rest of the heavy minerals. The Fe, Ni, and Cr are all ferrous elements and thus they display some correlation in the heavy mineral fraction.

The MEIS-II reflectance data for the test area do not have any significant correlation with the geochemical nature of the heavy mineral fraction of the basal till data.

The linear correlation for the same pair of elements in the two separate geochemical data sets, clay-sized fraction and heavy mineral fraction of the basal till is given in Table 8. From this table, it is obvious that there is generally a higher concentration of elements in the clay-sized fraction than in the heavy mineral fraction. This is probably due to the high ion exchange capacity of clay minerals, and thus they tend to adsorb different cations to the surface of the particles. It is possible that the extraction technique for heavy minerals did not release all the metals. For the same elemental analysis from different samples (the clay-sized fraction and heavy mineral fraction), there appears to be no correlation. This represents the different origins and geochemical nature of the two sample populations and thus the element concentrations in them significantly differ geochemically.

## CONCLUSIONS

The mineral exploration techniques involving geophysical, geochemical, geobotanical, biogeochemical, and remote sensing, have been used successfully in the past. Any mineral exploration approach which integrates all the different techniques is likely to increase the success rate in the mineral exploration and eventually have substantial economic benefits. Remote sensing particularly the airborne multispectral techniques that is, MEIS-II and MSS use narrow band spectral filters which are easily interchangeable and can provide an optimum combination of spectral windows for electromagnetic reflectance data. These airborne multispectral sensors with improved spatial and spectral resolution should be able to identify vegetation stresses effectively, which are caused by the anomalous concentrations of certain elements in the ground. Furthermore, these new techniques allow rapid acquisition of digital data for large areas, and the high speed of digital processing of the multispectral information is cost effective as compared to any of the ground-based exploration methods. Once the anomalies have been identified on the basis of remote sensing and airborne geophysical techniques, they can be further evaluated by ground-based methods. Thus the remote sensing approach can be used at the preliminary stage of the exploration to isolate the potential target areas.

Some of the more specific conclusions and recommendations learned from this experiment with regard to the MEIS-II and multispectral remote sensing study at the Farley Lake area are as follows:

1. The present airborne MEIS-II and MSS data indicate fairly low correlation with the biogeochemical data. These results, although not positive, have permitted us to develop several recommendations for future studies.



**Table 8.** Statistics of the till geochemical data, clay-sized fraction and heavy mineral fraction of the basal till data, Farley Lake area.

Element	Sample pair	Mean	Std. Dev.	Correlation coefficient
Copper	Clay fraction Heavy minerals	68.90	39.51	0.2103
Lead	Clay fraction Heavy minerals	7.28	7.200	-0.0386
Zinc	Clay fraction Heavy minerals	11.33	76.58	0.2056
Cobalt	Clay fraction Heavy minerals	8.55	22.99	-0.0742
Nickel	Clay fraction Heavy minerals	145.08	647.29	0.1655
Chromium	Clay fraction Heavy minerals	29.70	569.61	-0.0432
Manganese	Clay fraction Heavy minerals	15.66	4.98	0.0200
Iron	Clay fraction Heavy minerals	3.93	1.79	0.0567

\*Mean values are expressed in ppm except for iron which is expressed in percentage.

2. There is a positive correlation between the band 2 of MEIS-II data and iron concentration in the biogeochemical data at grid location 3. For the same grid band 1 and band 2 of the MEIS-II data display moderate correlation with the copper concentration.
3. Some of the factors which influence the spectral reflectance response of leaf and vegetation canopy have been identified, and a better understanding of these factors should lead to proper selection of spectral windows for the airborne multispectral MEIS-II and MS data acquisition.
4. In order to detect vegetation stress with remote sensors (airborne MEIS-II and MSS), the selection of narrow band spectral windows should be aided by a portable field spectrometer.
5. There is high correlation among the ferrous elements (i.e. Ni, Cr, Mn, and Fe), and the ferrous elements and zinc in the clay-sized fraction and the heavy mineral fraction of the basal till geochemical data.
6. The clay-sized fraction of basal till tends to have higher concentration of different elements as compared to the non-magnetic heavy mineral fraction for the same till sample. This is because the clay minerals have high cation exchange capacity and certain cations are adsorbed to the surface of the clay particles.

7. The relationship between different elements in the clay-sized fraction of basal till is the result of weathering and ionic mobility of elements in the aqueous phase.
8. The elemental concentrations in the clay-sized fraction of the till samples should be available to plants growing on the anomalously high concentrations of certain elements.
9. The geochemical analysis of the non-magnetic fraction of the heavy minerals in the till indicates the more resistant component of the till, whether derived from the underlying rocks or transported glacial overburden. The elemental compositions of the heavy mineral fraction were not affected by weathering and ionic mobility in the aqueous phase.
10. The analysis of heavy mineral fractions should help in interpretation of geochemical anomalies if there are any offsets due to the transport of glacial overburden.
11. Significant correlation exists between the Fe and Ni in the biogeochemical data of black spruce needles. The iron concentration is responsible for the darkening of needles.
12. The same elemental pairs in different biogeochemical grids do not show the same degree of linear correlation. This is due to a number of factors which influence the accumulation of elements in plants. Some of these factors have been identified in this study.
13. Due to the nature of the biogeochemical and geochemical sampling conducted in this area, it is difficult to determine the anomalous concentrations in the till samples that correspond to the anomalous concentrations in the plants.
14. The MEIS-II and MSS image data have a very high spatial resolution. Thus a mosaic produced from a combination of images may have a few million bytes of data even for a relatively small area. For this type of research, the computer hardware should have a large capacity disk storage, and sufficiently large memory.
15. Finally, the better understanding of the spectral reflectance properties of plants and biogeochemical behaviour of elements, will allow proper selection of 'narrow' band filters for the multispectral data acquisition and proper selection of elements to be used for the detection of biogeochemical anomalies. This type of approach could definitely prove to be a cost effective means of mineral exploration particularly in areas covered by thick vegetation and glacial overburden.

## REFERENCES

**Bateman, J.D.**

1945: McVeigh Lake area, Manitoba: Geological Surv. Canada Paper 45-14.

**Bolviken, B., Honey, F., Levine, S.R., Lyon, R.J.P., and Prelet, A.**

1977: Detection of naturally heavy-metal poisoned areas by Landsat 1 digital data: Jour. Geochem. Explor., v. 8, p. 457-471.

**Boyle, R.W., and McGerrigle, J.I. (eds)**

1971: Geochemical exploration: Proc. 3rd Internat. Geochem. Explor. Symp., Can. Inst. Min. Meta. Special v. 11, 594 p.

**Brooks, R.R.**

- 1972: Geobotany and Biogeochemistry in Mineral Exploration: Harper and Row Pub., 290 p.  
1983: Biological Methods of Prospecting for Minerals: John Wiley and Sons, 322 p.

**Cameron, E.M., (ed.)**

- 1966: Proceedings, symposium on geochemical prospecting, Ottawa, April 1966: Geological Surv. Canada Paper 66-54, 282 p.

**Chang, S., and Collins, W.**

- 1983: Confirmation of the airborne biogeophysical mineral exploration technique using laboratory methods: Economic Geology, v. 78, p. 723-736.

**Collins, W.S., Chang, S., Raines, G., Canney, F., and Ashley, R.**

- 1983: Airborne biogeophysical mapping of hidden mineral deposits: Economic Geology, v. 78, p. 737-749

**Colwell, J.E.**

- 1974: Vegetation canopy reflectance: Remote Sen. Environ., v. 3, p. 175-183.

**Cooley, W.W., and Lohnes, P.R.**

- 1971: Multivariate Data Analysis: John Wiley, 364 p.

**Corkery, M.T., and Lenton, P.G.**

- 1979: Lower Churchill River project in Manitoba: Mineral Resour. Div., Report of Field Act., GS-5, p. 47-57.

**Davis, J.C.**

- 1973: Statistics and Data Analysis in Geology: John Wiley, 550 p.

**DiLabio, R.N.W., Rencz, A.N., and Egginton, D.A.**

- 1982: Biogeochemical expression of a classic dispersion train of metalliferous till near Hopetown, Ontario: Can. Jour. Earth Sci. v. 19, p. 2297-2305.

**Eliason, P.T., Donovan, T.J. and Chavex, P.S. Jr.**

- 1983: Integration of geologic, geochemical and geophysical data of the Cement oil field, Oklahoma, using spatial array processing: Geophysics, v. 48, p. 1305-1317.

**Fedikow, M.A.F.**

- 1984: Preliminary results of biogeochemical studies in the Lynn Lake area: Geological Serv., Manitoba Energy and Mines, Open File Report OF84-1, 104 p.  
1985: The vegetation geochemical signature of the Agassiz stratabound Au-Ag deposit, Lynn Lake, Manitoba: Geological Serv., Manitoba Energy and Mines, Open File Report OF85-6.  
1986: Geology of the Agassiz stratabound Au-Ag deposits, Lynn Lake, Manitoba: Geological Serv., Manitoba Energy and Mines, Open File Report OF85-5.

**Fedikow, M.A.F. and Gale, G.H.**

- 1982: Mineral deposit studies in the Lynn Lake, area, in Manitoba Mineral Resour. Div. Report of Field Act., p. 44-54.

**Barrett, R.G.**

- 1971: The dispersion of copper and zinc in glacial overburden at Louvem deposit, Val d'Or, Quebec, in Boyle, R.W. and J.I. McGerrigle, (eds.); Geochemical exploration: Can. Inst. Min. Met. Special v. 11, p. 157-158.

**Gausman, H.W.**

1977: Reflectance of leaf components: *Remote Sen. Environ.*, v. 6, p. 1-9.

**Gilbert, H.P., Syme, E.C. and Swanzig, H.V.**

1980: Geology of metavolcanic and volcanoclastic metasedimentary rocks in the Lynn Lake area: *Manitoba Min. Resour. Div. Geological Paper GP 80-1*.

**Gleeson, C.F., and Cormier, R.**

1971: Evaluation by geochemistry of geophysical anomalies and geological targets using overburden sampling at depths, in Boyle, R.W., and J.I. McGerrigle, (eds.), *Exploration geochemistry: Can. Inst. Min. Met. Special v. 11, p. 159-165*.

**Goetz, A.F., Rock, B.N., and Rowan, L.C.**

1983: Remote sensing for exploration: an overview: *Economic Geology*, v. 78, p. 573-570.

**Guinness, E.A., Arvidson, R.E., Leff, C.E., Edwards, M.H., and Bindschadler, D.L.**

1983: Digital image processing applied to analysis of geophysical and geochemical data for southern Missouri: *Economic Geology*, v. 78, p. 654-663.

**Hawkes, H.E., and Webb, J.S.**

1962: *Geochemistry in Mineral Exploration: Harper and Row, 415 p.*

**Holer, D.N.H., Dockray, M., and Barber, J.**

1983: The red edge of plant leaf reflectance: *Int. Jour. Remote Sen.*, v. 4, p. 273-288.

**Horsnail, R.F., and Elliott, I.L.**

1971: Some environmental influences on secondary dispersion of molybdenum and copper in western Canada, in Boyle, R.W., and McGerrigle, J.I. *Geochemical exploration: Can. Inst. Meta. Special v. 11, p. 166-175*.

**Johnson, W.G.Q.**

1979: Compilation bedrock geology, Reindeer Lake south (NTS Area 64D) in Saskatchewan Geological Survey., *Summ. of Invest. 1977, Miscellaneous Report 79-10, p. 39-50*.

**Kettler, D., and Anderson, D.T.**

1986: An integrated remote sensing study of mineralized zones associated with the Agassiz Metallotect, Lynn Lake, Manitoba: a progress report: Unpublished report, 29 p.

**Labovitz, M.L., Masuoka, E.J., Bell, R., Siegrist, A.W., and Nelson, R.F.**

1983: The application of remote sensing to geobotanical exploration for metal sulfides—results from the 1980 field season at Mineral, Virginia: *Economic Geology*, v. 78, p. 750-760.

**Lulla, K.**

1985: Some observations on geobotanical remote sensing and mineral prospecting: *Can. Jour. Remote Sen.*, v. 11 p. 17-38.

**Milton, N.H.**

1983: Use of reflectance spectra of native plant species for interpreting airborne multispectral scanner data in the East Tintic mountains, Utah: *Economic Geology*, v. 78, p. 761-769.

**Morrison, D.F.**

1967: Multivariate Statistical Methods: McGraw-Hill, 338 p.

**Nielson, E., and Graham, D.C.**

1985: Preliminary results of till petrographical and till geochemical studies at Farley Lake: Geological Serv., Manitoba Energy and Mines, Open File Report OF85-3, 62 p.

**Nielson, E., and Fedikow, M.A.F.**

1986: Till geochemistry of the Minton Lake—Nikel Lake area (Agassiz Metalloctect), Lynn Lake, Manitoba: Geological Serv., Manitoba Energy and Mines, Open File Report OF86-2, 36 p.

**Norwood, V.T. and Lansing, J.C., Jr.**

1983: Electro-optical imaging sensors, in Colwell, R.N., (ed.), Manual of remote sensing, 2nd ed.,: Amer. Soc. Photogrammetry, v. 1, p. 335-367.

**Raines, G.L., and Canney, F.C.**

1980: Vegetation and geology, in Seigal, B.S., and A.R. Gillespie, (eds.), Remote Sensing in Geology: John Wiley, p. 365-380.

**Shilts, W.W.**

1975: Principles of geochemical exploration for sulphide deposits using shallow samples of glacial drift: Can. Inst. Min. Met. Bull., v. 68, p. 73-80.

1977: Geochemistry of till in perennially frozen terrain of the Canadian Shield, application to prospecting: Boreas, v. 5, p. 203-212.

1984: Till geochemistry in Finland and Canada: Jour. Geochem. Explor., v. 21, p. 95-117.

**Smith, J.A.**

1983: Matter-energy interaction in optical region, in Colwell, R.N., (ed.), Manual of remote sensing, 2nd ed.,: Amer. Soc. Photogrammetry, v. 1, p. 61-113.

**Sokal, R.R., and Sneath, P.H.A.**

1963: Principles of Numerical Taxonomy: W.H. Freeman and Co., San Francisco, 359 p.

**Tucker, C.J.**

1980: Remote sensing of leaf water content in the near-infrared: Remote Sen. Environ., v. 10, p. 23-32.

**Towmey, D.**

1977: Introduction to the Mathematics of Inversion in Remote Sensing and Indirect Measurements: Elsevier, 243 p.

**Westman, W.E., and Price, C.V.**

1988: Spectral changes in conifers subjected to air pollution and water stress: experimental studies: IEEE Trans. GRE, v. 26, p. 11-20.